A METHOD FOR THE IONOSPHERIC DELAY ESTIMATION AND INTERPOLATION IN A LOCAL GPS NETWORK

M.C. de Lacy[1], F. Sansò[2], A.J. Gil[1], G. Rodríguez-Caderot[3]

1 Dept. Ingeniería Cartográfica, Geodésica y Fotogrametría, Universidad de Jaén, Jaén, Spain (mclacy@ujaen.es)

2 Facoltà di Ingegneria di Como, Politecnico di Milano, Como, Italy (fernando.sanso@polimi.it)

3 Sec. Dptal. Astrononomía y Geodesia, Facultad de CC. Matemáticas, Universidad Complutense de Madrid, Madrid, Spain (grc@mat.ucm.es)

Received: November 13, 2003; Revised: June 19, 2004; Accepted: June 23, 2004

ABSTRACT

To estimate ionospheric delays from the Global Positioning System (GPS) measurements, satellite and receiver equipment biases have to be modeled. This paper presents a procedure based on the least squares (LS) approach, which implicitly takes into account these equipment biases in the estimation of the ionospheric effect. The second part of this work deals with the interpolation of the ionospheric correction from a permanent GPS network to a single frequency GPS user. The results obtained show that for 10-cm position accuracy the ionospheric delay can be successfully interpolated when the GPS user is within 40 km of the GPS permanent network.

Keywords: GPS, ionospheric delay, pseudorange electronic bias, interpolation

1. INTRODUCTION

GPS pseudorange and phase observations depend on the distance between satellite and receiver, ionospheric and tropospheric effects, satellite and receiver clock offsets, phase ambiguities, and satellite and receiver electronic biases. The main obstacle in the estimation of the ionospheric TEC (Total Electron Content) from dual frequency GPS data is the effect of the pseudorange electronic biases while the carrier phase equipment delays are absorbed by the ambiguity parameters.

A pseudorange bias is present for each of the two GPS frequencies and the difference between them is called differential code bias (DCB). Several authors have studied the problem of estimating the TEC and the differential code biases. *Coco et al. (1991)* represented the vertical TEC using polynomial coefficients. Three years later, *Sardon et al. (1994)* used a Kalman filtering approach to estimate the TEC and the DCBs. At the end of 1996, CODE (Center for Orbit Determination in Europe) began to produce daily global ionosphere maps (GIMs) using a spherical harmonic expansion to represent the TEC (http://www.aiub.unibe.ch/ionosphere). In 1999, *Schaer (1999)* studied the time series of the coefficients of the expansion into spherical harmonics used to represent the TEC.

Given the increased number of permanent GPS stations becoming available over the last years, the interpolation of ionospheric corrections from reference stations have been studied as part of the virtual GPS reference station concept by *Van der Marel (1999)* and more recently by *Odijk (2002)*. Obviously, studies have been of particular interest in the framework of RTK (Real Time Kinematic) positioning (*Fortes et al., 2003*).

In this paper, the ionospheric effect estimation from dual frequency GPS measurements is discussed. In Section 2, the dual frequency GPS observation equations are described. In Section 3, a procedure based on LS theory is combined with a global ionospheric model, such as the Klobuchar model or IGS ionospheric model, to estimate the ionospheric delay considering the differential electronic biases. In the second part, the perfomance of the ionospheric corrections, estimated and interpolated from GPS reference stations to a single frequency GPS user in an area encompassed by the network, is tested. In particular, this method is applied to two test data sets. The first data set is from an observation campaign of a GPS network established in southern Spain to monitor crustal deformation. The second is from the Lombard permanent GPS network in Italy. In both cases, rather short observation periods are used. The reason is that we are trying to simulate a "service" provided to a single frequency GPS user who typically tries to minimize the observation time for each station. The results are presented in Section 4.

2. OBSERVATION EQUATIONS AND THE EULER-GOAD MODEL

In the sequel we shall consider the following model for GPS carrier phase and pseudorange observables specific to a dual frequency receiver j and a satellite i (i.e., for undifferenced data) for a generic epoch t (*Teunissen and Kleusberg, 1998*):

$$\begin{aligned} P_{1j}^{i} = {} & \left|\left(\underline{x}^{i}\left(t-\tau_{j}^{i}\right)+\underline{dx}_{1}^{i}\left(t-\tau_{j}^{i}\right)\right)-\left(\underline{x}_{j}(t)+\underline{dx}_{1j}(t)\right)\right|+J_{1j}^{i}+T_{j}^{i} \\ & +c\left[dt^{i}\left(t-\tau_{j}^{i}\right)-dt_{j}(t)\right]+c\left[d_{1}^{i}\left(t-\tau_{j}^{i}\right)+d_{1j}(t)\right]+dm_{1j}+\varepsilon_{1} \end{aligned}$$

$$\begin{aligned} P_{2j}^{i} = {} & \left|\left(\underline{x}^{i}\left(t-\tau_{j}^{i}\right)+\underline{dx}_{2}^{i}\left(t-\tau_{j}^{i}\right)\right)-\left(\underline{x}_{j}(t)+\underline{dx}_{2j}(t)\right)\right|+J_{2j}^{i}+T_{j}^{i} \\ & +c\left[dt^{i}\left(t-\tau_{j}^{i}\right)-dt_{j}(t)\right]+c\left[d_{2}^{i}\left(t-\tau_{j}^{i}\right)+d_{2j}(t)\right]+dm_{2j}+\varepsilon_{2} \end{aligned}$$

$$\begin{aligned} L_{1j}^{i} \equiv \frac{-c\Phi_{1j}^{i}}{f_{1}} = {} & \left|\left(\underline{x}^{i}\left(t-\tau_{j}^{i}\right)+\underline{\delta x}_{1}^{i}\left(t-\tau_{j}^{i}\right)\right)-\left(\underline{x}_{j}(t)+\underline{\delta x}_{1j}(t)\right)\right|+J_{1j}^{i}+T_{j}^{i} \\ & +c\left[dt^{i}\left(t-\tau_{j}^{i}\right)-dt_{j}(t)\right]+c\left[\delta_{1}^{i}\left(t-\tau_{j}^{i}\right)+\delta_{1j}(t)\right]+\delta m_{1j} \\ & +\lambda_{1}N_{1j}^{i}+\lambda_{1}\left[\phi_{1}^{i}(t_{0})-\phi_{1j}(t_{0})\right]+\varepsilon_{3} \end{aligned}$$

$$L_{2j}^{i} \equiv \frac{-c\Phi_{2j}^{i}}{f_2} = \left| \left(\underline{x}^{i}\left(t-\tau_j^{i}\right) + \underline{\delta x}_2^{i}\left(t-\tau_j^{i}\right)\right) - \left(\underline{x}_j(t) + \underline{\delta x}_{2j}(t)\right)\right| + J_{2j}^{i} + T_j^{i}$$
$$+c\left[dt^{i}\left(t-\tau_j^{i}\right) - dt_j(t)\right] + c\left[\delta_2^{i}\left(t-\tau_j^{i}\right) + \delta_{2j}(t)\right] + \delta m_{2j} \tag{1}$$
$$+\lambda_2 N_{2j}^{i} + \lambda_2\left[\phi_2^{i}(t_0) - \phi_{2j}(t_0)\right] + \varepsilon_4$$

where P_{1j}^{i} and P_{2j}^{i} are the code pseudoranges; Φ_{1j}^{i} and Φ_{2j}^{i} are the recorded carrier phases; L_{1j}^{i} and L_{2j}^{i} are the carrier phases expressed as ranges; $\underline{x}^{i}$ is the position vector of the centre of mass of the satellite; $\underline{x}_j$ is the position vector of the terrestrial point; $\underline{dx}_k^{i}$ is the eccentricity vector of the transmitting antenna phase center relative to the pseudorange measurements at frequency f_k; $\underline{dx}_{kj}$ represents the eccentricity vector of the receiver antenna relative to the pseudorange measurements at frequency f_k; $\underline{\delta x}_k^{i}$ is the eccentricity vector of the transmitting antenna phase center pertaining to the carrier phase measurements at frequency f_k; $\underline{\delta x}_{kj}$ represents the eccentricity vector of the receiver antenna phase center pertaining to the carrier phase measurements at frequency f_k.

In general, the eccentricities relative to pseudoranges and carrier phases are different since the effective antenna phase centers are different.

τ_j^{i} is the signal travel time from the signal generator in the satellite to the signal correlator in the GPS receiver. τ_j^{i} can be split into three separate terms: the signal delay d^{i} occurring between the signal generation in the satellite and the transmission from the satellite antenna, the signal travel time $\delta\tau_j^{i}$ from the transmitting antenna to the receiver antenna, and the signal delay d_j between the receiving antenna and the signal correlator in the receiver, $\tau_j^{i} = d^{i} + \delta\tau_j^{i} + d_j$; $c\left[d_k^{i}\left(t-\tau_j^{i}\right) + d_{kj}(t)\right]$ is tested pseudorange satellite and receiver equipment delay at frequency f_k or a pseudorange electronic bias; $c\left[\delta_k^{i}\left(t-\tau_j^{i}\right) + \delta_{kj}(t)\right]$ carrier phase satellite and receiver equipment delay at frequency f_k or carrier phase electronic biases; J_{kj}^{i} ionospheric delay effect at frequency f_k; T_j^{i} the tropospheric delay effect; dt^{i} and dt_j satellite and receiver clock offset, respectively; dm_{kj}^{i} pseudorange multipath at frequency f_k; δm_{kj}^{i} carrier phase multipath at frequency f_k; $\lambda_k\left[\phi_k^{i}(t_0) - \phi_{kj}(t_0)\right]$ is a constant term that represents the non-zero initial phases of the satellite and receiver generated signals; N_{kj}^{i} are the integer carrier phase ambiguities at frequency f_k; ε_1, ε_2, ε_3, ε_4 are the measurement noises; c = 299792458 m/s is the speed of light.

The GPS system frequencies used in the above equations are the following: $f_1 = 154 \times f_0$ Hz; $f_2 = 120 \times f_0$ Hz, with f_0 = 10230000 Hz; $\lambda_1 = c/f_1$, $\lambda_2 = c/f_2$.

Some approximations can be assumed in Eqs.(1) in order to express them in a more suitable form:

1. The differences between the frequency dependent pseudorange and carrier antenna phase centers (both in receiver and satellites) are neglected. Therefore, the geometric distance between the satellite antenna and receiver antenna can be written as:

$$D_j^i = \left| \left(\underline{x}^i + \underline{dx}^i \right) - \left(\underline{x}_j + \underline{dx}_j \right) \right|, \tag{2}$$

that is to say, this geometric distance is assumed to be independent of the frequency and is the same for pseudoranges and carrier phases.
2. The multipath terms and electronic biases are ignored.
3. It is possible to distinguish between frequency-dependent and non-dispersive terms. The satellite-receiver distance, the clock terms and the tropospheric delay belong to the last group. They can be lumped together into one single term:

$$\rho_j^i = D_j^i + c\left(dt^i - dt_j \right) + T_j^i \tag{3}$$

This term would also include any other delay which affects all data identically, such as the effect of selective availability (SA).

The frequency dependent part can be split into two terms: the ionospheric delay effect at frequency f_k that is approximated by the first order term of a Taylor series expansion; and the ambiguity biases b_{kj}^i. This last term is formed by lumping together the non-zero initial phases and the integer carrier phase ambiguities, that is:

$$b_{1j}^i = \left[\phi_1^i(t_0) - \phi_{1j}(t_0) \right] + N_{1j}^i, \; b_{2j}^i = \left[\phi_2^i(t_0) - \phi_{2j}(t_0) \right] + N_{2j}^i. \tag{4}$$

Keeping in mind these simplifications, Euler and Goad wrote the carrier phase and pseudorange observables specific to a receiver-satellite pair for a generic epoch in the following way (*Goad, 1985*):

$$\begin{cases} P_{1j}^i(t) = \rho_j^i(t) + J_{1j}^i(t) + \varepsilon_1 \\ P_{2j}^i(t) = \rho_j^i(t) + KJ_{1j}^i(t) + \varepsilon_2 \\ L_{1j}^i(t) = \rho_j^i(t) - J_{1j}^i(t) + \lambda_1 b_{1j}^i + \varepsilon_3 \\ L_{2j}^i(t) = \rho_j^i(t) - KJ_{1j}^i(t) + \lambda_2 b_{2j}^i + \varepsilon_4 \end{cases}, \tag{5}$$

where $K = \left(f_1/f_2 \right)^2$.

It is important to stress that each of the equations in (5) is known to be biased by a constant term which represents the travel time of the signal through the circuitries of the receiver and satellite. The main source of error in the estimation of TEC (Total Electron Content) from dual frequency GPS data is the effect of these electronic biases. It is known that the combined receiver and satellite DCBs can be up to several nanoseconds. *Sardon and Zarraoa (1997)* studied DCB stability from day to day. They found a variation in the GPS satellite biases relative to the mean of less than 0.1 ns, while for the receiver the difference between estimates in consecutive days is below 1 ns. As a consequence for short periods of time, for example one hour, we can consider the electronic biases to be constant.

3. ESTIMATION OF THE IONOSPHERIC EFFECT

3.1. A mathematical model taking into account the differential code biases

Since our goal is to estimate the ionospheric delay, we consider the Eqs.(5) introducing the pseudo-range electronic biases Q_{1j}^i and Q_{2j}^i:

$$Q_{1j}^i = c\left(d_1^i + d_{1j}\right),\ Q_{2j}^i = c\left(d_2^i + d_{2j}\right), \tag{6}$$

and lumping together the carrier phase electronic biases, integer ambiguity and the non-zero initial phases of the satellite and receiver into B_{1j}^i and B_{2j}^i, defined as:

$$B_{1j}^i = \lambda_1 b_{1j}^i + c\left(\delta_1^i + \delta_{1j}\right),\ B_{2j}^i = \lambda_2 b_{2j}^i + c\left(\delta_2^i + \delta_{2j}\right), \tag{7}$$

that is,

$$\begin{cases} P_{1j}^i(t) = \rho_j^i(t) + J_{1j}^i(t) + Q_{1j}^i + \varepsilon_1 \\ P_{2j}^i(t) = \rho_j^i(t) + KJ_{1j}^i(t) + Q_{2j}^i + \varepsilon_2 \\ L_{1j}^i(t) = \rho_j^i(t) - J_{1j}^i(t) + B_{1j}^i + \varepsilon_3 \\ L_{2j}^i(t) = \rho_j^i(t) - KJ_{1j}^i(t) + B_{2j}^i + \varepsilon_4 \end{cases}. \tag{8}$$

We can consider the observations as a function of time during a period of n_t epochs. To remove the differential code biases we multiply these observations by ($\mathbf{I} - \mathbf{Pe}$), where $\mathbf{I}$ is the identity natrix and $\mathbf{Pe}$ is the projector, $\mathbf{Pe} = \frac{1}{n_t}\underline{e}\,\underline{e}^t$, with $\underline{e} = (1,1,\ldots 1)^t$. In this way, the mathematical model specific to a receiver i and a satellite j will be:

$$\begin{cases} \underline{V}_{P1} = (\mathbf{I}-\mathbf{Pe})\underline{P}_{1j}^{i} = (\mathbf{I}-\mathbf{Pe})\underline{\rho}_{j}^{i} + (\mathbf{I}-\mathbf{Pe})\underline{J}_{1j}^{i} \\ \underline{V}_{P2} = (\mathbf{I}-\mathbf{Pe})\underline{P}_{2j}^{i} = (\mathbf{I}-\mathbf{Pe})\underline{\rho}_{j}^{i} + K(\mathbf{I}-\mathbf{Pe})\underline{J}_{1j}^{i} \\ \underline{V}_{\Phi_1^i} = (\mathbf{I}-\mathbf{Pe})\underline{L}_{1j}^{i} = (\mathbf{I}-\mathbf{Pe})\underline{\rho}_{j}^{i} - (\mathbf{I}-\mathbf{Pe})\underline{J}_{1j}^{i} \\ \underline{V}_{\Phi_2^i} = (\mathbf{I}-\mathbf{Pe})\underline{L}_{2j}^{i} = (\mathbf{I}-\mathbf{Pe})\underline{\rho}_{j}^{i} - K(\mathbf{I}-\mathbf{Pe})\underline{J}_{1j}^{i} \end{cases} . \tag{9}$$

In the least squares (LS) adjustment our unknown parameters become ρ_j^i, J_j^i; the vectorization of the various quantities above is accomplished with respect to the index t (time). If we put:

$$\begin{cases} (\mathbf{I}-\mathbf{Pe})\underline{\rho}_{j}^{i} = \underline{\eta} \\ (\mathbf{I}-\mathbf{Pe})\underline{J}_{j}^{i} = \underline{\lambda} \end{cases} , \tag{10}$$

indeed these parameters share the property

$$\begin{cases} \underline{e}^{t} \cdot \underline{\eta} = 0 \\ \underline{e}^{t} \cdot \underline{\lambda} = 0 \end{cases} . \tag{11}$$

As we have projected our observations into the manifold of the admissible values for the observables, we can assume that the stochastic model associated with Eq.(9) is given by

$$\mathbf{C} = \sigma_0^2 \begin{pmatrix} \mathbf{Q}_{P1} & 0 & \dots & 0 \\ 0 & \mathbf{Q}_{P2} & 0 & 0 \\ 0 & 0 & \mathbf{I}_{n_t \times n_t} & 0 \\ 0 & 0 & \dots & \mathbf{I}_{n_t \times n_t} \end{pmatrix} , \tag{12}$$

where $\mathbf{Q}_{Pk} = \mathrm{diag}(q_k, q_k, \ldots, q_k)$, with $k = 1,2$ and $\dim \mathbf{Q}_{Pk} = n_t \times n_t$. We have considered $\sigma_0^2 = 0.002^2\,\mathrm{m}^2$, $q_1 = 10^5$ and $q_2 = 10^4$. This is equivalent to a noise of 60 cm for the P1 code and 20 cm for the P2 code. The noise of code observations depends on the receiver. In non-cross-correlation receivers, both codes present the same level of accuracy. However in cross-correlation receivers the noise of one code is bigger than the other. We chose the above values in order to represent the most pessimistic situation. Of course, such values are fairly pessimistic with respect to present perfomances and even more to the results expected in a few years. However, to avoid making our error estimates of ionospheric delays too optimistic, we prefer to be as conservative as is reasonably necessary.

Applying the LS theory, our problem is reduced to finding the minimum of the function:

$$\theta\left(\underline{\hat{\eta}},\underline{\hat{\lambda}}\right)=\frac{1}{2}\left(q_1^{-1}\left|\underline{V}_{P1}-\underline{\hat{\eta}}-\underline{\hat{\lambda}}\right|^2+q_2^{-1}\left|\underline{V}_{P2}-\underline{\hat{\eta}}-K\underline{\hat{\lambda}}\right|^2\right.$$
$$\left.+\left|\underline{V}_{\Phi_1}-\underline{\hat{\eta}}+\underline{\hat{\lambda}}\right|^2+\left|\underline{V}_{\Phi_2}-\underline{\hat{\eta}}+K\underline{\hat{\lambda}}\right|^2\right), \tag{13}$$

where q_1^{-1} and q_2^{-1} are the inverse of the diagonal elements of the weight matrix; $\underline{\hat{\eta}}$ and $\underline{\hat{\lambda}}$ are the LS estimator of $\underline{\eta}$ and $\underline{\lambda}$, respectively.

Computing the partial derivates of θ with respect to $\underline{\hat{\eta}}$ and $\underline{\hat{\lambda}}$, equalling them to zero we find the following system:

$$\begin{cases}\left(2+q_1^{-1}+q_2^{-1}\right)\underline{\hat{\eta}}- \\ -\left(1+K-q_1^{-1}-q_2^{-1}K\right) & = \quad q_1^{-1}\underline{V}_{P1}+q_2^{-1}\underline{V}_{P2}+\underline{V}_{\Phi_1}+\underline{V}_{\Phi_2} \\ \\ -\left(1+K-q_1^{-1}-q_2^{-1}K\right)\underline{\hat{\eta}}+ \\ +\left(1+K^2+q_1^{-1}+q_2^{-1}K^2\right)\underline{\hat{\lambda}} & = \quad q_1^{-1}\underline{V}_{P1}+q_2^{-1}K\underline{V}_{P2}-\underline{V}_{\Phi_1}-\underline{V}_{\Phi_2}\end{cases} . \tag{14}$$

Writing this system in matrix form, we get:

$$\mathbf{A}\begin{pmatrix}\underline{\hat{\eta}} \\ \underline{\hat{\lambda}}\end{pmatrix}=\mathbf{B}\begin{pmatrix}\underline{V}_{P1} \\ \underline{V}_{P2} \\ \underline{V}_{\Phi_1} \\ \underline{V}_{\Phi_2}\end{pmatrix}, \tag{15}$$

with:

$$\mathbf{A}=\begin{pmatrix}\left(2+q_1^{-1}+q_2^{-1}\right) & -\left(1+K-q_1^{-1}-q_2^{-1}K\right) \\ -\left(1+K-q_1^{-1}-q_2^{-1}K\right) & \left(1+K^2+q_1^{-1}+q_2^{-1}K^2\right)\end{pmatrix} \tag{16}$$

and:

$$\mathbf{B}=\begin{pmatrix}q_1^{-1} & q_2^{-1} & 1 & 1 \\ q_1^{-1} & q_2^{-1}K & -1 & -K\end{pmatrix}. \tag{17}$$

Finally, the LS solution we are looking for is:

$$\begin{pmatrix} \hat{\underline{\eta}} \\ \hat{\underline{\lambda}} \end{pmatrix} = \mathbf{A}^{-1}\mathbf{B} \begin{pmatrix} \underline{V}_{P1} \\ \underline{V}_{P2} \\ \underline{V}_{\Phi_1} \\ \underline{V}_{\Phi_2} \end{pmatrix} = \begin{pmatrix} \alpha_{P1}\underline{V}_{P1} + \alpha_{P2}\underline{V}_{P2} + \alpha_{\Phi_1}\underline{V}_{\Phi_1} + \alpha_{\Phi_2}\underline{V}_{\Phi_2} \\ \beta_{P1}\underline{V}_{P1} + \beta_{P2}\underline{V}_{P2} + \beta_{\Phi_1}\underline{V}_{\Phi_1} + \beta_{\Phi_2}\underline{V}_{\Phi_2} \end{pmatrix}, \tag{18}$$

where:

$$\mathbf{A}^{-1}\mathbf{B} = \begin{pmatrix} \alpha_{P1} & \alpha_{P2} & \alpha_{\Phi_1} & \alpha_{\Phi_2} \\ \beta_{P1} & \beta_{P2} & \beta_{\Phi_1} & \beta_{\Phi_2} \end{pmatrix}. \tag{19}$$

A procedure based on LS theory to solve the Euler-Goad equations is explained in Appendix. One interesting point is to write the solution as we have done in this Appendix, that is to say one can trace explicitly where and how the electronic biases end up in the estimates of smoothed pseudoranges $\hat{\rho}_j^i(t)$ and of the ionospheric delays $\hat{J}_{1j}^i(t)$. It is important to note that the difference between the solution given by Eq.(18) and Eq.(A18) minus the mean of Eq.(A18) is at 0.1 mm level.

Applying the covariance propagation law, the covariance matrices of the unknown parameters are obtained:

$$\begin{aligned} \mathbf{C}_{\hat{\underline{\eta}}\hat{\underline{\eta}}} &= \alpha_{P1}^2\sigma_{P1}^2(\mathbf{I}-\mathbf{Pe}) + \alpha_{P2}^2\sigma_{P2}^2(\mathbf{I}-\mathbf{Pe}) + \alpha_{\Phi_1}^2\sigma_{\Phi_1}^2(\mathbf{I}-\mathbf{Pe}) + \alpha_{\Phi_2}^2\sigma_{\Phi_2}(\mathbf{I}-\mathbf{Pe}) \\ &= \sigma_{\Phi_1}^2\left(\alpha_{P1}^2 q_1 + \alpha_{P2}^2 q_2 + \alpha_{\Phi_1}^2 + \alpha_{\Phi_2}^2\right)(\mathbf{I}-\mathbf{Pe}) \end{aligned} \tag{20}$$

$$\begin{aligned} \mathbf{C}_{\hat{\underline{\lambda}}\hat{\underline{\lambda}}} &= \beta_{P1}^2\sigma_{P1}^2(\mathbf{I}-\mathbf{Pe}) + \beta_{P2}^2\sigma_{P2}^2(\mathbf{I}-\mathbf{Pe}) + \beta_{\Phi_1}^2\sigma_{\Phi_1}^2(\mathbf{I}-\mathbf{Pe}) + \beta_{\Phi_2}^2\sigma_{\Phi_2}(\mathbf{I}-\mathbf{Pe}) \\ &= \sigma_{\Phi_1}^2\left(\beta_{P1}^2 q_1 + \beta_{P2}^2 q_2 + \beta_{\Phi_1}^2 + \beta_{\Phi_2}^2\right)(\mathbf{I}-\mathbf{Pe}) \end{aligned} \tag{21}$$

It can be observed that in both cases the covariance matrices do not depend on time and Eqs.(20) and (21) numerically coincide with the first term of Eq.(A20).

3.2. An approach to modelling the ionospheric effect

From the above paragraph we have obtained $\hat{\underline{\lambda}} = (\mathbf{I}-\mathbf{Pe})\underline{J}_{1j}^i$. This means, the estimate of the difference between the ionospheric effect at each epoch minus the mean of the ionospheric correction over the observation period. In order to obtain the estimate of the ionospheric correction at each epoch we propose to model this mean as the mean of an ionospheric model; in our case we have used the Klobuchar model (*Leick, 1995*) and the ionosphere model implied by IONEX TEC MAPS (ftp://cddisa.gsfc.nasa.gov/gps/products/ionex). In this way, the estimate of the ionospheric effect, $\hat{\underline{I}}_j^i$, between a single receiver j and a single satellite i is given by:

$$\underline{\hat{I}}_j^i = \left((\mathbf{I} - \mathbf{Pe}) \underline{J}_{1j}^i \right) + \overline{\text{mod}}_j^i , \tag{22}$$

with

$$\overline{\text{mod}}_j^i = \frac{1}{n_t} \sum_{t=1}^{n_t} \text{mod}_j^i (t) , \tag{23}$$

where $\text{mod}_j^i(t)$ is the ionospheric delay between the receiver j and the satellite i computed from an ionospheric model. Of course, the errors in this model may propagate into our solution. However since the model is good at long wavelengths and the average operator further smooths out such errors, we expect acceptable results from such an approach.

The procedure explained in this section has been implemented. First results obtained from this method are presented in this paper. As the main goal of the work is to study whether or not a permanent GPS network could provide the ionospheric correction to single frequency GPS users, the first tests regarding the interpolation of Eq.(22) have been carried out and are presented in the next section.

4. FIRST RESULTS AND DISCUSSION

4.1. The dataset

In 1999 a GPS network was established to monitor the crustal deformations in the Granada Basin (south of Spain, *Gil et al., 2002*). GPS surveys were carried out in 1999, 2000 and 2001. In this work, a GPS data set belonging to session 175 (23 June 2000) was used to test the procedure explained in Section 3. In Fig. 1 the distribution of points within the network for session 175 can be seen. For our numerical tests we have supposed that this configuration corresponds to a hypothetical GPS network where points 5, 8, 25 and 22 are considered as permanent GPS stations and point 11 represents a single frequency GPS user. The following summarizes the data set used:

- Day: 23-06-2000.
- Observation time span: from 15:40:00 to 16:19:45 UTC.
- Sample rate: 15 seconds.
- Cut-off angle: 15°.
- Dual frequency phase and code receivers. In particular, Leica SR399 receiver with internal antennae at points 8, 22 and 25 and SR9500 receiver with external antennae AT302 at points 5 and 11.
- Satellites tracked by all stations: PRN 1,PRN 4, PRN 16, PRN 18, PRN 19, PRN 27.
- No cycle slips and outliers are present in the data set.
- The precise coefficients α and β of the Klobuchar model determined by Code analysis center (http://www.aiub.unibe.ch/download/CODE).

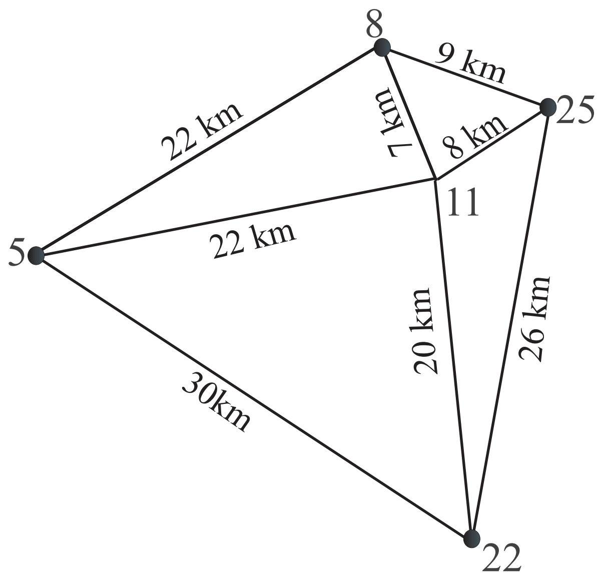

Fig. 1. GPS reference network (5,8,25,22) and GPS user (11).

4.2. Estimation of the ionospheric delay

As we mentioned above we aim to test the perfomance of the ionospheric correction interpolated from the GPS reference stations to a single frequency GPS user inside the test area. To do this, we have developed three steps:

1. The ionospheric effect was estimated by Eq.(22) at each epoch, at each GPS reference station (point 5, 8, 22 and 25) and interpolated to a single frequency GPS user placed at the point 11. The behaviour of the ionospheric delay was studied. In particular, the values obtained at station 5 with some satellites are plotted in Fig. 2. In this case, the mean of the model (23) was computed using the precise Klobuchar coefficients from CODE center.
2. The ionospheric delay at point 11 was obtained by interpolating the ionospheric delays estimated at the GPS reference stations. A weighted mean, with weights proportional to the inverse of the distance between the GPS user and the reference station, was used for interpolation.
3. The residual ionospheric effect was computed to determine the quality of the interpolator. This residual is the difference between "interpolated" and "real" ionospheric effect, where "real" corresponds to the delay computed from Eq.(22). In Fig. 3 the values of the residuals are presented.

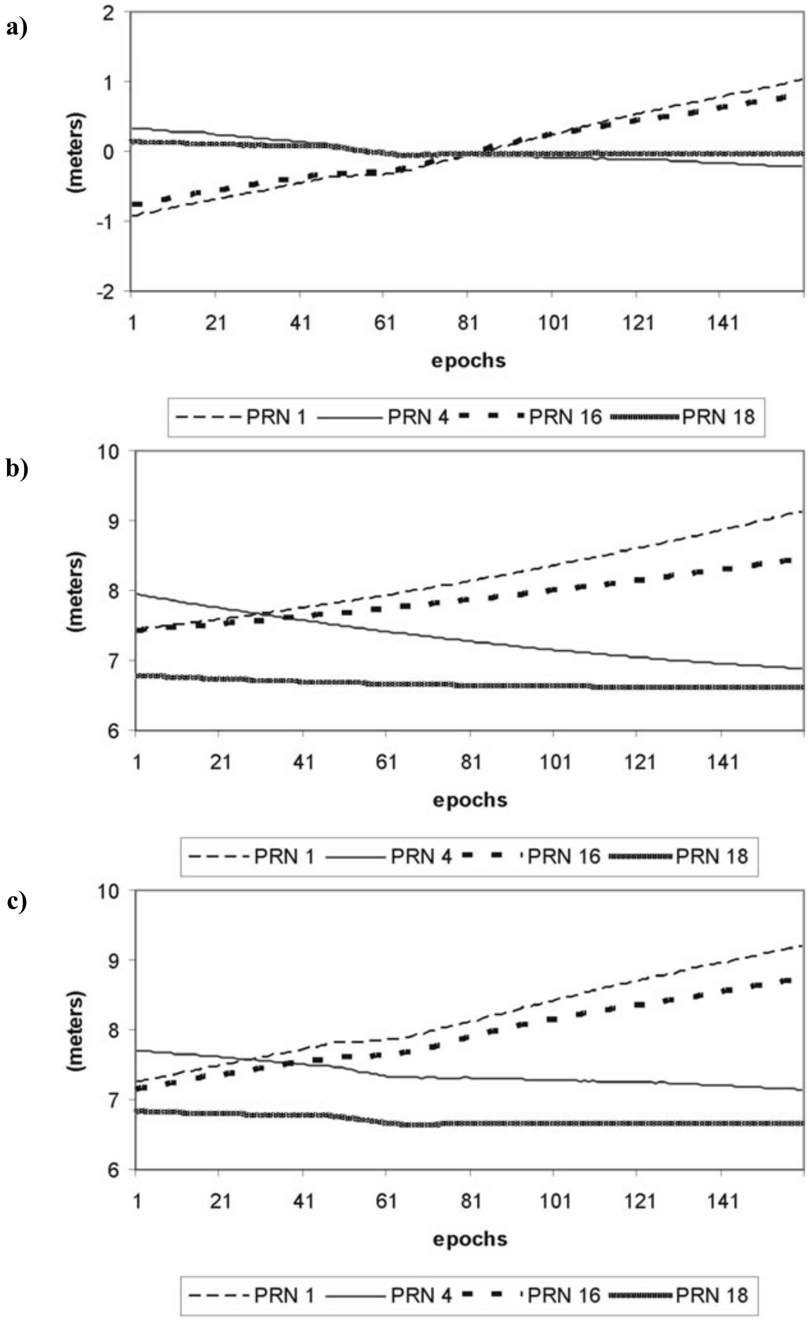

Fig. 2. Ionospheric delay at Station 5. **a)** Biased ionospheric delay implied by Eq.(18). **b)** Global ionospheric model. **c)** Total ionospheric delay implied by Eq.(22).

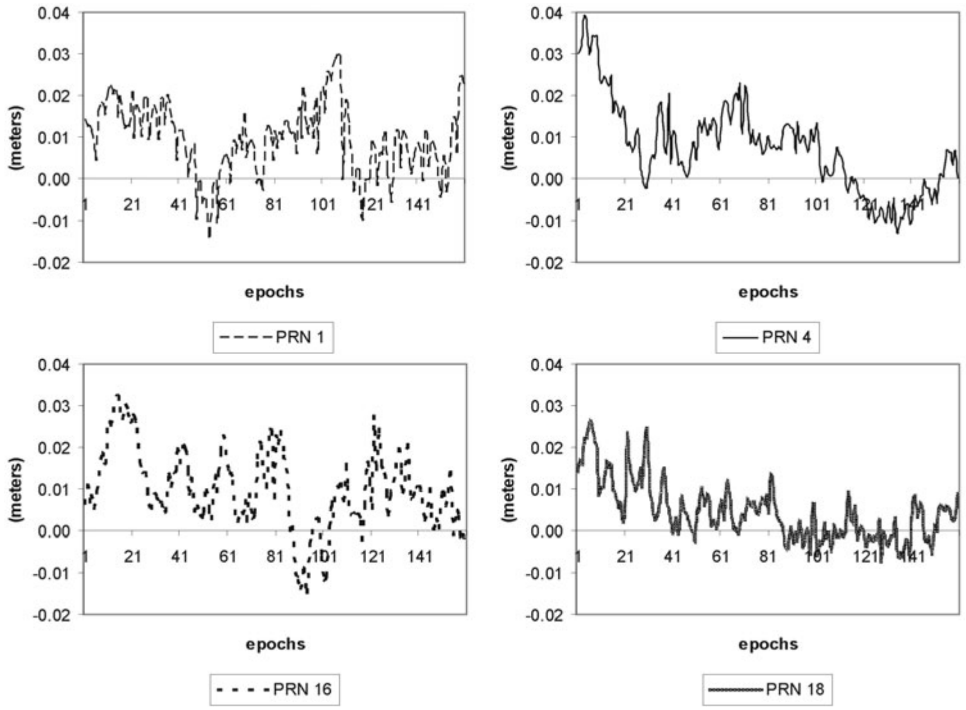

Fig. 3. Residual ionospheric effect: the difference between interpolated and “real” ionospheric effects, where “real” corresponds to the delay computed from Eq.(22).

Fig. 2 is composed of three parts: the left column represents the values generated by Eq.(18), Fig. 2b shows the ionospheric effect stemming from the precise Klobuchar model coefficients, and Fig. 2c represents the total ionospheric delay computed from Eq.(22). It can be observed that the Klobuchar model is very smooth and contributes the “order of magnitude” to the mean of the ionospheric delay in Eq.(22). In Fig. 2a, the values range up to one meter and contribute to generating the “details” of the ionospheric delay given by Eq.(22). Regarding residuals (Fig. 3), it can be observed that all residuals are less than 4 cm.

4.3. Influence on baseline processing

In order to further test the perfomance of the ionospheric delay interpolator in terms of efficiency for baseline determination, baseline differences with respect to the known solution were analysed using four different ways of correcting for the ionosphere. First, the ionospheric delay was estimated by the Klobuchar model with broadcast and precise coefficients. After that, the ionosphere correction was estimated by Eq.(22) considering two different global models: the Klobuchar model with precise coefficients α and β, and the ionosphere model implied by IONEX TEC maps. In the latter case the values of TEC in our observation time were obtained by interpolating two consecutive rotated maps and applying a simple 4-point formula to interpolate the grid points. To do this, the Fortran routines available from ftp://ftp.unibe.ch/unibe/ionex/source were used. GPS measurements were processed with the GPSurvey software (*Trimble, 1999*) in the following way:

- Observations: P1, L1 free of cycle slips.
- Ephemerides: precise.
- Troposphere: Saastamoinen model with standard atmosphere parameters.
- Ionosphere: Klobuchar model and ionospheric delay estimated by Eq.(22). In the latter case the observations were corrected using Eq.(22) and then processed with GPSurvey software without the ionospheric model option.
- Antenna offsets provided by the International GPS Service (IGS).
- Solution: L1 ambiguities fixed, when possible.

From our geodynamic GPS network, including many more baselines and sessions, we have derived what we consider to be the “true” beseline components. They can be seen in Table 1. The results of the baseline processing are shown in Table 2. The first column identifies the baseline considered. The second one gives the difference between “true” baseline components and the baseline components obtained using only the broadcast Klobuchar model to estimate the ionosphere effect. The fourth shows the difference between “true” baseline components and the baseline components obtained using only the precise Klobuchar coefficients (determined by CODE) to estimate the ionosphere effect. The sixth shows the difference between “true” baseline components and the baseline components obtained estimating the ionosphere delay using Eq.(22), using the Klobuchar model with the precise coefficients as a global model. Column number eight gives the difference between “true” baseline components and the baseline components obtained estimating the ionosphere delay using Eq.(22), using the ionosphere model implied by IONEX TEC maps to compute the mean (23). In the adjacent columns, the type of solution obtained by GPSurvey software, i.e floating or fixed, for each particular case, is also given.

From Table 2 we can conclude:

- The results improve when IGS products are used.
- In general, the differences between “true” values and estimated values are smaller when we model the ionospheric effect using Eq.(22).
- No substantial differences were found when we modeled the ionosphere with Eq.(22) using the precise Klobuchar model and the IGS ionosphere model implied by IONEX TEC maps.
- When we estimated the ionospheric effect using Eq.(22), the L1 fixed solution was achieved in three cases. However, using the broadcast Klobuchar model only, we obtained a fixed solution for the baseline 22-11, but the differences with “true” values were large. This suggests that the ionospheric effect implied by Eq.(22) represents the ionosphere better than the Klobuchar model.

The final test carried out to study the quality of the ionospheric interpolation is to adjust the above baselines to estimate the coordinates of point 11. In Table 3 the coordinates obtained from this adjustment are shown. Taking into account the above results (no substantial differences between columns six and eight in Table 2) the precise Klobuchar model was used in Eq.(22). It can be seen again that the adjusted coordinates

Table 1. "True" baseline components (session 175).

Baseline	*X* [m]	*Y* [m]	*Z* [m]
25-11	2597.452	–5998.385	–7760.937
22-11	–12158.208	–1347.419	16061.456
5-11	–768.754	22274.197	3350.074
8-11	4533.845	2660.82	–5666.414

Table 2. Baseline Processing. *TC* = "True" components. *KC*(1) = Components estimated using only the broadcast Klobuchar model. *KC*(2) = Components estimated using the precise Klobuchar model only. *EC*(1) = Components estimated with the ionospheric delay given by Eq.(22) using the precise Klobuchar model to compute the mean (23). *EC*(2) = Components estimated with the ionospheric delay given by Eq.(22) using the IGS model implied by IONEX TEC maps to compute the mean (23).

Baseline		*TC–KC*(1)	Solution	*TC–KC*(2)	Solution	*TC–EC*(1)	Solution	*TC–EC*(2)	Solution
25-11	ΔX	0.077	L1 float	0.030	L1 fixed	0.042	L1 fixed	0.027	L1 fixed
	ΔY	0.031		0.008		0.001		0.008	
	ΔZ	0.078		0.032		0.018		0.017	
22-11	ΔX	–0.108	L1 fixed	–0.098	L1 float	0.046	L1 float	0.045	L1 float
	ΔY	–0.151		–0.067		0.045		0.043	
	ΔZ	–0.113		–0.136		0.034		0.033	
5-11	ΔX	0.123	L1 float	0.127	L1 float	0.093	L1 fixed	0.083	L1 fixed
	ΔY	0.114		0.085		–0.043		–0.046	
	ΔZ	0.089		0.100		0.015		0.021	
8-11	ΔX	0.102	L1 fixed	0.068	L1 fixed	0.048	L1 fixed	0.063	L1 fixed
	ΔY	0.004		0.004		0.007		0.002	
	ΔZ	0.071		0.056		0.044		0.048	

are better when IGS products are used. The differences between "true" coordinates and estimated coordinates are better than 6 cm and the differences between the two last solutions are not statistically significant. This is probably due to the distribution of the points in this session.

4.4. Dataset belonging to the Lombard GPS permanent network

A project to establish a permanent GPS network in Lombardy (North of Italy) is being developed (see Fig. 4). GPS observations from Como (Co), Milano Agraria (Mi), Pavia (Pv) and Brescia (Br) permanent stations were used to test the perfomance of our

Table 3. Coordinate estimation of point 11. For meaning of *TC*, *KC*(1), *KC*(2) and *EC*(1), see Table 1.

Solution	*X* [m]	St. Dev [m]	*Y* [m]	St. Dev [m]	*Z* [m]	St. Dev [m]
TC	5077851.788		–318413.099		3835122.585	
KC(1)	5077851.708	±0.018	–318413.101	±0.010	3835122.523	±0.010
KC(2)	5077851.742	±0.015	–318413.106	±0.006	3835122.544	±0.008
EC(1)	5077851.731	±0.026	–318413.094	±0.010	3835122.553	±0.013

approach in a larger area. The following summarizes the data set and baseline processing strategy:

- Day: 16-01-2003.
- Two observation sessions: from 10:00:00 to 10:30:00 UTC and from 14:20:00 to 14:50:00 UTC.
- Sample rate: 1 second in Como, Pavia, Milano and 5 seconds in Brescia.
- Cut-off angle: 10°.
- Dual frequency phase and code receivers. Specifically Trimble 4000ssi with antenna choke rings in Como and Brescia, Ashtech Z12 with antenna Geodetic IIIA in Milan and TRIMBLE 4700 with antenna choke ring in Pavia.
- Ephemerides: rapid ephemerides from IGS. The choice of using the rapid ephemerides instead of the precise ones was due to the fact that for such short bases and short time spans, no substantial differences in the results were found.
- Troposphere: Saastamoinen model with standard atmosphere parameters.
- Ionosphere: precise Klobuchar model only and ionospheric delay estimated by Eq.(22) using the IGS ionospheric model implied by IONEX TEC map. In the latter case, the observations were corrected using Eq.(22) and then the ionospheric delays were interpolated to estimate the ionopheric effect in Milan. Finally, observations were processed with GPSurvey software without the ionospheric model option.
- Antenna offsets provided by the International GPS Service (IGS).
- Solution: L1 ambiguities fixed, when possible.

The ionospheric effect resulting from our approach was interpolated to a fictitious single GPS user located at Milan station using a weighted mean, with weights proportional to the inverse of the distance between the GPS user and the permanent station. Subsequently, the baselines Pv-Mi, Co-Mi and Br-Mi were processed and adjusted to estimate the coordinates of the fictitious GPS user inside the area defined by the permanent stations. The baseline solutions using the ionosphere effect modeled by the precise Klobuchar model and by Eq.(22) are shown in Tables 5 and 6. They were compared with the baselines computed from the ETRF89 coordinates of the points (see Table 4) considered as “true” values. In Tables 5 and 6 it can be seen that the differences with the “true” values are smaller when our approach is used. The improvement is really great when we processed the longer baselines. This suggests that our approach gives a

Fig. 4. Lombard GPS permanent network (Italy).

more faithful representation of the ionosphere. Furthermore, the STD (standard deviation) of solutions obtained using Eq.(22) is always smaller than that implied by the precise Klobuchar model. The adjusted coordinates of the single frequency GPS user are computed using the GPS network module of the GPSurvey software. The geographical coordinates are shown in Table 7. It can be seen that the STD of the coordinates provided by our method are better than 4 cm and is always smaller than the solution implied by the precise Klobuchar model. Furthermore the results show that the height estimated by our approach is better than that estimated using the precise Klobuchar model only.

In summary, the ionosphere delay can be interpolated and broadcast over a larger GPS network; in our particular case the method worked when the distance between the GPS single frequency user and a permanent station was about 70 km. To confirm this result, more tests should be carried out. From a conservative point of view, we can say that the method works when the distance between the GPS single frequency user and a permanent station is under 40 km and accuracies better than 10 cm are required.

Table 4. ETRF89 baseline slope distance [m].

Pv-Mi	31203.660
Co-Mi	37633.557
Br-Mi	79188.494

Table 5. Baseline slope distance [m] estimated using the precise Klobuchar model.

Base	Base Estimation	STD	Solution	Difference from "True" Value
Pv-Mi (session 1)	31203.526	0.039	float	0.134
Pv-Mi (session 2)	31203.691	0.026	float	–0.031
Co-Mi (session 1)	37633.658	0.068	float	–0.101
Co-Mi (session 2)	37633.694	0.022	float	–0.137
Br-Mi (session 1)	79188.668	0.099	float	–0.174
Br-Mi (session 2)	79188.361	0.107	float	0.133

Table 6. Baseline slope distance [m] estimated with the ionospheric delay, given by Eq.(22), using the IGS model implied by IONEX TEC maps to compute the mean (23).

Base	Base Estimation	STD	Solution	Difference from "True" Value
Pv-Mi (session 1)	31203.560	0.036	float	0.100
Pv-Mi (session 2)	31203.702	0.023	float	–0.042
Co-Mi (session 1)	37633.652	0.032	float	–0.095
Co-Mi (session 2)	37633.500	0.019	float	0.056
Br-Mi (session 1)	79188.554	0.033	float	–0.060
Br-Mi (session 2)	79188.570	0.054	float	–0.076

Table 7. Coordinate estimation of GPS user inside the test area. TC = "True" Coordinates. KC(2) = Coordinates estimated using the precise Klobuchar model. EC(2) = Coordinates estimated with the ionospheric delay, given by Eq.(22), using the IGS model implied by IONEX TEC maps to compute the mean (23).

Solution	Latitude	STD [m]	Longitude	STD [m]	*H* [m]	STD [m]
TC	45°28′34.828061″		+9°13′36.911848″		174.100	
KC(2)	45°28′34.828786″	±0.051	+9°13′36.912958″	±0.110	174.046	±0.064
EC(2)	45°28′34.828522″	±0.020	+9°13′36.909835″	±0.039	174.102	±0.027

5. CONCLUSIONS

The problem of estimating the ionospheric effect from dual frequency GPS measurements has been studied in this paper. A procedure based on LS theory is combined with a global ionosphere model to estimate the ionospheric correction implicitly taking the differential code biases into account. The procedure has the advantage that it can work with observations from a single GPS station. This is particularly useful for a permanent GPS array because it allows the direct ionospheric estimation based on a station by station approach without the heavier computational burden resulting from processing all the stations at once. The estimated ionospheric effect has been interpolated from GPS reference stations to a single frequency GPS user within two test areas. In the first test, a GPS network composed of short baselines was considered. The ionospheric effect was estimated, interpolated and compared with the "real" ionospheric effect over a short period. The residuals obtained were always less than 4 cm. In the second test, a data set from the GPS permanent Lombard network was used. The ionospheric delay estimated and interpolated was then used to estimate the coordinates of a single frequency GPS point. Our results prove that modeling the ionosphere effect with our procedure gives better results than when using only a global model such as the Klobuchar model with precise coefficients determined by the CODE analysis center. This means that the differences between baseline estimated and "true" values are smaller when our method is used. Furthermore, the STD of our solutions are also smaller than those implied by the global model. From our results, we can conclude that the ionospheric effect can be successfully estimated and interpolated to a GPS single frequency user inside a permanent GPS network if the the distance between the GPS user and GPS permanent stations is less than 40 km.

APPENDIX

If we consider the deterministic part of the model (5), which the LS estimates have to satisfy, we can construct the inverse relation between our four unknown parameters and the observables at each epoch t.In particular we can write:

$$\underline{\hat{b}} = \begin{pmatrix} \hat{b}_{1j}^{i} \\ \hat{b}_{2j}^{i} \end{pmatrix} = \mathbf{R}\underline{\hat{y}}_t , \tag{A1}$$

$$\underline{\hat{\xi}}_t = \begin{pmatrix} \hat{\rho}_j^i(t) \\ \hat{J}_{1j}^i(t) \end{pmatrix} = \boldsymbol{\Gamma}\underline{\hat{y}}_t , \tag{A2}$$

where $\underline{\hat{y}}_t$ denotes the LS estimator of the observation vector at epoch t and

$$\mathbf{R} = \begin{pmatrix} \frac{-(1+K)}{K-1} & \frac{2}{K-1} & 1 & 0 \\ \frac{-2K}{K-1} & \frac{K+1}{K-1} & 0 & 1 \end{pmatrix}, \tag{A3}$$

$$\boldsymbol{\Gamma} = \begin{pmatrix} \frac{K}{K-1} & \frac{-1}{K-1} & 0 & 0 \\ \frac{-1}{K-1} & \frac{+1}{K-1} & 0 & 0 \end{pmatrix}. \tag{A4}$$

Then, the problem to be solved reads:

$$\min \sum_{t=1}^{n_t} \left(\underline{y}_{ot} - \underline{\hat{y}}_t \right)^T \mathbf{P} \left(\underline{y}_{ot} - \underline{\hat{y}}_t \right), \tag{A5}$$

$$\begin{cases} \underline{\hat{\xi}}_t = \mathbf{\Gamma} \underline{\hat{y}}_t \\ \underline{\hat{b}} = \mathbf{R} \underline{\hat{y}}_t \end{cases}, \tag{A6}$$

where $\mathbf{P} = \mathbf{Q}^{-1}$ with

$$\mathbf{C} = \sigma_0^2 \mathbf{Q} = \sigma_0^2 \begin{pmatrix} q_1 & 0 & 0 & 0 \\ 0 & q_2 & 0 & 0 \\ 0 & 0 & 1 & 0 \\ 0 & 0 & 0 & 1 \end{pmatrix}, \tag{A7}$$

in which we have considered $\sigma_0^2 = 0.002^2$ m^2, $q_1 = 10^5$ and $q_2 = 10^4$. This is equivalent to a noise of 60 cm for the P1 code and 20 cm for the P2 code.

It is important to note that the first equation in (A6) is directly used to estimate the smoothed pseudorange and ionospheric delay parameters at each epoch, while the second is used to define the manifold of admissible values for the observables.

To solve the problem (A5) we form the Lagrange function

$$W\left(\underline{\hat{y}}_t, \underline{\hat{b}} \right) = \frac{1}{2} \sum_{t=1}^{n_t} \left(\underline{y}_{ot} - \underline{\hat{y}}_t \right)^T \mathbf{P} \left(\underline{y}_{ot} - \underline{\hat{y}}_t \right) + \sum_{t=1}^{n_t} \underline{\lambda}_t^T \left(\underline{\hat{b}} - \mathbf{R} \underline{\hat{y}}_t \right). \tag{A8}$$

To minimize this function, the derivatives respective to $\underline{\hat{y}}_t$ and $\underline{\hat{b}}$ are set equal to zero and then we solve the equation system formed by adding the second condition of (A6):

$$\begin{cases} -\mathbf{P} \left(\underline{y}_{ot} - \underline{\hat{y}}_t \right) - \mathbf{R}^T \underline{\lambda}_t = 0 \\ \sum_{t=1}^{n_t} \underline{\lambda}_t^T = 0 \\ \underline{\hat{b}} = \mathbf{R} \underline{\hat{y}}_t \end{cases}. \tag{A9}$$

From the first equation:

$$\underline{y}_{ot} - \underline{\hat{y}}_t = -\mathbf{Q} \mathbf{R}^T \underline{\lambda}_t . \tag{A10}$$

Substituting in the third one, we obtain:

$$\underline{\hat{b}}_t = \mathbf{R} \underline{y}_{ot} + \mathbf{K} \underline{\lambda}_t , \tag{A11}$$

where $\mathbf{K} = \mathbf{RQR}^T$. Then, the parameter $\underline{\lambda}_t$ is:

$$\underline{\lambda}_t = \mathbf{K}^{-1}\left(\hat{\underline{b}} - \mathbf{R}\underline{y}_{ot}\right). \tag{A12}$$

From the second equation:

$$\sum_{t=1}^{n_t} \mathbf{K}^{-1}\left(\hat{\underline{b}} - \mathbf{R}\underline{y}_{ot}\right) = 0 . \tag{A13}$$

Therefore,

$$n_t \mathbf{K}^{-1}\hat{\underline{b}} - \mathbf{K}^{-1}\mathbf{R}\sum_{t=1}^{n_t} \underline{y}_{ot} = 0 . \tag{A14}$$

Finally, we obtain the LS ambiguity bias estimate:

$$\hat{\underline{b}} = \frac{1}{n_t}\mathbf{R}\sum_{t=1}^{n_t} \underline{y}_{ot} = \mathbf{R}\underline{\overline{y}}_o . \tag{A15}$$

Substituting now (A15) in (A12), we have:

$$\underline{\lambda}_t = -\mathbf{K}^{-1}\mathbf{R}\left(\underline{y}_{ot} - \underline{\overline{y}}_o\right). \tag{A16}$$

Putting $\underline{\lambda}_t$ in (A10), we can write:

$$\hat{\underline{y}}_t = \underline{y}_{ot} - \mathbf{QR}^T\mathbf{K}^{-1}\mathbf{R}\left(\underline{y}_{ot} - \underline{\overline{y}}_o\right). \tag{A17}$$

Substituting (A17) in (A2) we obtain the LS pseudorange and inospheric delay solutions at each epoch:

$$\begin{aligned}\hat{\underline{\xi}}_t &= \mathbf{\Gamma}\left(\mathbf{I} - \mathbf{QR}^T\mathbf{K}^{-1}\right)\underline{y}_{ot} + \mathbf{\Gamma}\mathbf{QR}^T\mathbf{K}^{-1}\mathbf{R}\underline{\overline{y}}_o \\ &= \mathbf{\Gamma}\underline{y}_{ot} - \mathbf{\Gamma}\mathbf{QR}^T\mathbf{K}^{-1}\mathbf{R}\left(\underline{y}_{ot} - \underline{\overline{y}}_o\right).\end{aligned} \tag{A18}$$

From this expression we can see, as promised, how the electronic biases influence the estimates $\hat{\underline{\xi}}_t = \left(\hat{\rho}(t)\ \hat{J}(t)\right)^T$. In fact, the term $\underline{y}_{ot} - \underline{\overline{y}}_o$ is clearly bias free so that the biases enter only through the first term $\mathbf{\Gamma}\underline{y}_{ot}$ and due to the particular form of $\mathbf{\Gamma}$ we see that the phase biases play no role at all while the (larger) pseudorange biases (Q_1 and Q_2) enter into $\hat{\rho}(t)$ as $\frac{KQ_1 - Q_2}{K-1}$ and into $\hat{J}(t)$ as $\frac{Q_2 - Q_1}{K-1}$. In particular, it is this last term which is taken from a global ionospheric model.

To obtain the covariance matrices of the LS parameters, we apply the law of covariance propagation. In this way,

$$\mathbf{C}_{\underline{\hat{b}}\underline{\hat{b}}} = \frac{1}{n_t}\mathbf{RCR}^T \text{, with } \mathbf{C} = \sigma_0^2\mathbf{Q} . \tag{A19}$$

$$\begin{aligned}\mathbf{C}_{\underline{\hat{\xi}}_t \underline{\hat{\xi}}_t} &= \delta_{tt'}\boldsymbol{\Gamma}\left(\mathbf{I}-\mathbf{CR}^T\mathbf{K}^{-1}\mathbf{RC}\right)\mathbf{C}\left(\mathbf{I}-\mathbf{R}^T\mathbf{K}^{-1}\mathbf{RC}\right)\boldsymbol{\Gamma}^T \\ &+\frac{1}{n_t}\left(\mathbf{I}-\mathbf{CR}^T\mathbf{K}^{-1}\mathbf{R}\right)\mathbf{CR}^T\mathbf{K}^{-1}\mathbf{RC}\boldsymbol{\Gamma}^T \\ &+\frac{1}{n_t}\boldsymbol{\Gamma}\mathbf{CR}^T\mathbf{K}^{-1}\mathbf{RC}\left(\mathbf{I}-\mathbf{R}^T\mathbf{K}^{-1}\mathbf{RC}\right)\boldsymbol{\Gamma}^T \\ &+\frac{1}{n_t}\boldsymbol{\Gamma}\mathbf{CR}^T\mathbf{K}^{-1}\mathbf{RCR}^T\mathbf{K}^{-1}\mathbf{RC}\boldsymbol{\Gamma}^T\end{aligned} \tag{A20}$$

with

$$\delta_{tt'} = \begin{cases} 1 & \text{if} \quad t = t' \\ 0 & \text{if} \quad t \neq t' \end{cases} . \tag{A21}$$

Acknowledgements: The authors thank the reviewers for their valuable suggestions which have improved this paper.

References

Coco D.S., Coker C., Dahlke S.R. and Clynch J.R., 1991. Variability of GPS satellite differential group delay biases. *IEEE Trans. Aerosp. Electron. Syst.*, **7**, 931–938.

Fortes L.P., Cannon M.E., Lachapelle G. and Skone S., 2003. Optimizing a network-based RTK method for OTF positioning. *GPS Solutions*, **7**, 61–73.

Gil A.J., Rodríguez-Caderot G., de Lacy M.C., Ruiz A., Sanz de Galdeano C. and Alfaro P., 2002. Establishment of a non permanenet GPS Network to Monitor the Deformation in Granada Basin (Betic Cordillera, Southern Spain). *Stud. Geophys. Geod.*, **46**, 395–410.

Goad C.C., 1985. Precise relative position determination using Global Positioning System carrier phase measurements in undifference mode. *Proceedings of the First Symposium on Precise Positioning with the Global Positioning System, Positioning with GPS-1985*, U.S. Department of Commerce, NOOA, USA, 347–356.

Leick A., 1995. *GPS Satellite Surveying*. John Wiley & Sons, Hoboken, New Jersey, USA.

Odijk D., 2002. *Fast Precise GPS Positioning in the Presence of Ionospheric Delays*. *NCG Series*, **52**, Netherlands Geodetic Commission, Delft, The Netherlands.

Sardon E. and Zarraoa N., 1997. Estimation of total electron content using GPS data: How stable are the differential satellite and receiver instrumental biases? *Radio Sci.*, **32**, 1899–1910.

Sardon E., Rius A. and Zarraoa N., 1994. Estimation of the transmitter and receiver differential biases and the ionospheric total electron content from Global Positioning System observations. *Radio Sci.*, **29**, 577–586.

Schaer S., 1999. Mapping and Prediction the Earth's Ionosphere Using the Global Positioning System. *Geodaetisch-geophysikalische Arbeiten der Schweiz*, **59**, Swiss Geodetic Commission, Swiiss Academy of Sciences, Bern, Switzerland.

Teunissen P.J.G. and Kleusberg A., 1998. *GPS for Geodesy, 2nd Edition.* Springer-Verlag, Heidelberg, Germany.

Trimble, 1999. GPSurvey, version 2.35a. Trimble Navigation Ltd.

van der Marel H., 1998. Virtual GPS Reference Station in the Netherlands. *ION GPS-98 Proceedings of the 11th International Technical Meeting of the Satellite Division of the Institute of Navigation*, Institute of Navigation, Fairfax, VA, USA, 49–58.